Gait verification using knee acceleration signals

L.W. Hang [a,b], C.Y. Hong [c], C.W. Yen [c,*], D.J. Chang [c], M.L. Nagurka [d]

[a] Sleep Medicine Center, Department of Internal Medicine, China Medical University Hospital, Taichung, Taiwan
[b] Department of Healthcare Administration, Asia University, Taichung, Taiwan
[c] Department of Mechanical and Electro-mechanical Engineering, National Sun Yat-sen University, Kaohsiung, Taiwan
[d] Department of Mechanical Engineering, Marquette University Milwaukee, WI 53201, USA

ARTICLE INFO

ABSTRACT

A novel gait recognition method for biometric applications is proposed. The approach has the following distinct features. First, gait patterns are determined via knee acceleration signals, circumventing difficulties associated with conventional vision-based gait recognition methods. Second, an automatic procedure to extract gait features from acceleration signals is developed that employs a multiple-template classification method. Consequently, the proposed approach can adjust the sensitivity and specificity of the gait recognition system with great flexibility. Experimental results from 35 subjects demonstrate the potential of the approach for successful recognition. By setting sensitivity to be 0.95 and 0.90, the resulting specificity ranges from 1 to 0.783 and 1.00 to 0.945, respectively.

© 2011 Elsevier Ltd. All rights reserved.

1. Introduction

The goal of a biometric system is to identify or verify a person using individual physiological or behavioral characteristics (Jain, Ross, & Prabhakar, 2004; Xiao, 2007; Zhang & Zuo, 2007). Many biometric features, such as electrocardiograms (Chan, Hamdy, Badre, & Badee, 2005), fingerprints (Girgis, Sewisy, & Mansour, 2009; Hong, Min, Cho, & Cho, 2008), gait (Lee, Hong, & Kim, 2009; Tao, Li, Wu, & Maybank, 2007), heart sound (Phua, Chen, Dat, & Shue, 2008), iris (Chen & Chu, 2009; Rakshit & Monro, 2007), palmprint (Huang, Jia, & Zhang, 2008; Su, 2009), signature (Impedovo & Pirlo, 2008; Nanni, Maiorana, Lumini, & Campisi, 2010), typing dynamics (Araújo, Sucupira, Liźarraga, Ling, & Yabu-Uti, 2005), vein (Wang, Leedham, & Cho, 2008; Wu & Ye, 2009) and voice (Wahab, Ng, & Dickiyanto, 2005; Wang, Yang, Wang, & Lee, 2007) have been proposed. Among these biometric features, gait has the following distinct properties. First, gait recognition can be processed unobtrusively. Second, gait is difficult to disguise. Third, since the mean comfortable walking speed is approximately 51.5 strides per minute (Bussmann, Damen, & Stam, 2000), one can obtain hundreds of gait cycle samples in a few minutes. This feature is significant since the success of the design and validation of a pattern recognition system depends strongly on the sample size (Dass, Zhu, & Jain, 2007; Raudys & Jain, 1991; Sordo & Zeng, 2005).

Most current gait biometric systems use cameras to capture gait information (Boulgouris & Chi, 2007; Boulgouris, Hatzinakos, & Plataniotis, 2005; Lee et al., 2009; Nixon & Carter, 2006; Sarkar et al., 2005; Tao et al., 2007; Xu et al., 2006; Zhang, Vogler, & Metaxas, 2007). After separating the walking person from the background, gait features are extracted from the image sequence. The success of these vision-based gait recognition systems depends on several critical factors. First, to be most effective, the subject needs to walk in a direction perpendicular to the optical axis of the camera (Boulgouris et al., 2005). Second, to achieve accurate person-environment separation, the background needs to be as uniform and as time-invariant as possible (Sarkar et al., 2005). Imperfect person-environment separation introduces noise into the gait features that degrades the recognition rate. Third, the accuracy of the gait recognition is significantly limited by the distance between the subject and the camera (Zhang et al., 2007). In summary, the sensitivity to environmental variations, capturing angle of the camera, and the distance between the subject and camera make vision-based gait recognition systems difficult to implement in many real-world situations.

In additional to the optical motion analysis methods, accelerometers have been used in gait research in many studies to determine kinematic and kinetic information (Bogert van den, Read, & Nigg, 1996; Hayes, Gran, Nagurka, Feldman, & Oatis, 1983; Kavanagh, Morrison, James, & Barrett, 2006). Accelerometer-based gait recognition methods have also been proposed (Gafurov, Snekkenes, & Bours, 2007; Mäntyjärvi, Lindholm, Vildjiounaite, Mäkelä, & Ailisto, 2005). By directly measuring the hip acceleration, these approaches acquire gait features without the need for cumbersome image processing techniques. The sensitivity to the environmental factors, such as background complexity and the appearance of other persons, is thus avoided.

In comparison to methods that utilize hip acceleration signals, this study relies on knee acceleration information to characterize

* Corresponding author. Tel.: +886 7 342965; fax: +886 7 5254299.
E-mail address: cmurobot@gmail.com (C.W. Yen).

the gait pattern. This change gives rise to two additional benefits. First, accelerometer-measured knee signals can be used to diagnose the health of the knee joint (Krishnan, Rangayyan, Bell, & Frank, 2000; McCoy, McCrea, Beverland, Kernohan, & Mollan, 1987). This can be a significant advantage since the knee joint is the most commonly injured or diseased joint in the body (Rangayyan & Wu, 2008). Second, knee-mounted devices have been developed to harvest energy from a person's stride (Andrysek & Chau, 2007; Donelan et al., 2008). By collecting the kinetic energy that would otherwise be dissipated at the end of the swing phase, such devices can generate an average of 5 W of electricity from each leg. (Such power is sufficient to operate 10 typical cell phones simultaneously.) By integrating such a device with an accelerometer, one can easily design a self-charging sensor that can simultaneously perform long-term knee health monitoring and identity verification.

Another important unique feature of this study is the use of a hyperspherical classifier (Telfer & Casasent, 1993) to explore the potential of drawing on a large number of gait samples to enhance the recognition accuracy. By varying its parameters, the sensitivity and specificity of the hyperspherical classifier can be systematically adjusted to improve the overall gait recognition rate.

The paper is organized as follows. The following section describes the hardware setup and introduces the proposed feature extraction method. Section 3 illustrates a systematic approach for hyperspherical classifier design. Section 4 presents the experimental results, and a discussion and conclusion are given in Section 5.

2. Gait feature extraction

2.1. Hardware setup

The motion sensor employed in this work is a three-dimensional accelerometer (Analog Devices ADXL330, ±3 g range, sensitivity 330 mV/g). The size of the accelerometer is 4 mm × 4 mm × 1.45 mm. In attaching the accelerometer to the knee of all tested subjects, the x, y and z-axes of the sensor were aligned with the anterior-posterior, medial-lateral and proximal-distal directions, respectively. The acceleration signal was transmitted wirelessly to a notebook computer. The z-axis component of the acceleration (denoted as A_z hereafter) was recorded with a 12-bit National Instruments (NI) USB-6008 data acquisition card at a 1 kHz sampling rate. In every recording session, each subject was asked to walk approximately forty steps. The data was recorded indoors in a 40 m tiled hallway. Fig. 1 depicts a typical example of A_z after removing the DC component of the signal.

2.2. Extraction process

The first part of the feature extraction process is to remove the transitional part of the A_z which consists of the initial and final portions of each walking session. This is accomplished by the following procedure.

(1) By observing the peaks of A_z in every gait cycle, determine a parameter P to represent the nominal value of such peaks.
(2) Find every local maximum for A_z.
(3) Determine the first local maximum that is larger than P and remove the portion of A_z that comes ahead of this local maximum.
(4) Similarly, determine the last local maximum that is larger than P and remove the portion of A_z that comes after this local maximum.

The second part of the feature extraction process is to divide A_z into a number of gait cycles by finding the end of the swing phase
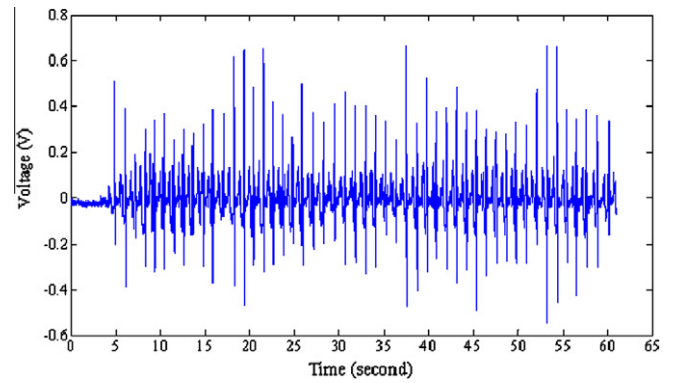

Fig. 1. A typical accelerometer output time response.

in every gait cycle. This is accomplished by applying the following procedure:

(1) Filter A_z by removing its frequency component above 1.5 Hz. Fig. 2a and b depict a typical A_z before and after such an operation, respectively. Note that the peaks that appear in every gait cycle of the original A_z correspond to heel-strike.
(2) Determine the local maxima for the filtered A_z. These local maxima correspond to the end of the swing phase in every gait cycle. However, as shown in Fig. 2b, the low-pass filtering operation has suppressed the magnitude and shifted the time-of-occurrence of the heel-strike peaks. The goal of the following two steps is to recover the true time-of-occurrence of these peaks in order to accurately divide A_z into a number of gait cycles.
(3) After finding the time differences between every pair of neighboring local maxima of the filtered A_z, find the median (denoted as L) of these time differences.
(4) Let t_i represent the time associated with the ith local maxima for the filtered A_z. Find an absolute maximum of the original A_z from the time interval $t_i - 0.2L \leqq t \leqq t_i + 0.2L$, where t is the time variable. The time associated with such an absolute maximum is denoted as T_i.
(5) Assign the time interval between every pair of T_i and T_{i+1} as a gait cycle.
(6) Normalize each gait cycle to 1000 sampling points via linear interpolation. The ith time-normalized gait cycle is denoted as G_i in the remaining part of this paper.
(7) The variation of many uncontrollable factors such as shoes and walking surface may alter the magnitude of A_z. Therefore, the third step of the feature extraction process
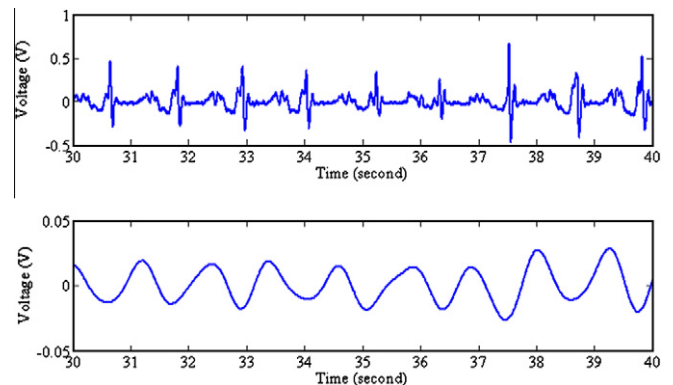

Fig. 2. The accelerometer output responses before and after the low-pass filtering operation.
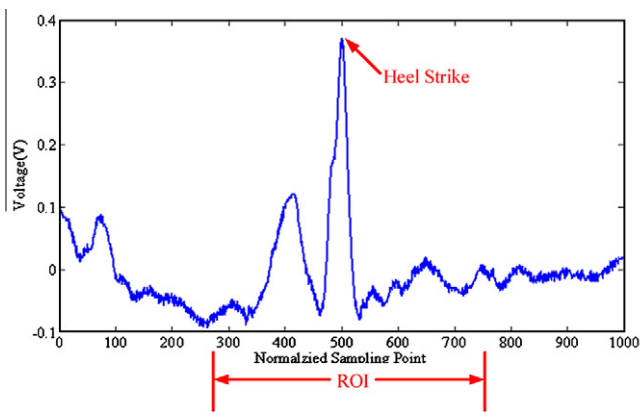
Fig. 3. Determining the region of interest (ROI) from the neighborhood region of heel strike.

is to normalize A_z so that the average power of every G_i is equal to unity for every gait recording session.

The final part of the proposed feature extraction method is to determine the feature vector by finding the region of interest (ROI) for each gait cycle. In this study, ROI is selected from the portion of A_z near the heel-strike since the interpersonal differences of such an interval seem to be more significant than the remaining part of A_z. As shown in Fig. 3, heel-strike occurs at the central part of the gait cycle. Therefore, the time of heel-strike can be determined by finding the maximum value of A_z between the 250th and the 750th sampling points of the time-normalized G_i. With the time of heel-strike as the center, the ROI is selected as a 501-sample-point subinterval of the normalized gait cycle. After down-sampling this ROI with a factor of 10, an ROI vector of dimension 50 can be acquired from each gait cycle. Finally, to enhance the reliability of the recognition system, a gait feature vector is obtained by averaging the ROI vectors from five walking steps.

3. Hyperspherical classifier design

Previously reported accelerometer-based gait recognition systems used template-based techniques to perform gait recognition. By comparing the similarity between the tested feature vector and a pre-stored template, the decision of rejection or acceptance is made based on a "matching score" between these two vectors. However, considering the magnitude and diversity of the possible variations of human biometric traits, accurate recognition may require multiple templates (Jain et al., 2004).

Fig. 4 presents an example of the distribution pattern of an artificial two-dimensional biometric feature vector that illustrates the
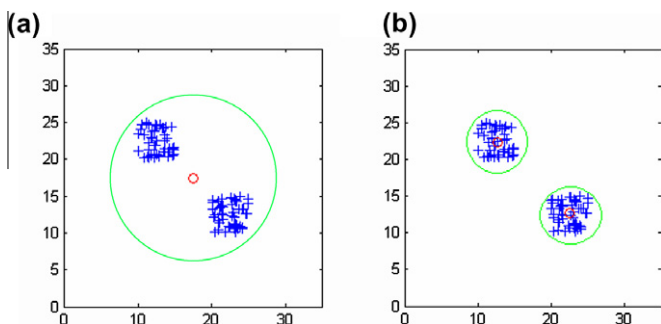

Fig. 4. Acceptance regions for (a) a single hypersphere and (b) two hypersphere classifiers.

advantages of multiple templates. With the mean of the samples as the template and the Euclidean distance as the similarity measure, the acceptance region is constructed as a circle. The false acceptance (rejection) error can be improved (degenerated) by decreasing (increasing) the radius of this circle. As a result, the sensitivity and specificity of this recognition system can be adjusted systematically. The key weakness of this single-template approach is the redundancy of the acceptance region since, as shown in Fig. 4a, the shape of the true acceptance region is very different from a circle.

This problem can be partially resolved by using two templates, as demonstrated in Fig. 4b. When circles can be properly placed, the redundancy of the acceptance region can be reduced further by increasing the number of circles. Based on this concept, several hyperspherical classifier design methods have been proposed to tackle classification problems of higher dimension (Telfer & Casasent, 1993; Yen & Liu, 1997). A drawback of these approaches is that their algorithms require the setting of a number of ad hoc parameters which may influence the convergence of the design process. Another challenge of these methods is in the difficulty in balancing the sensitivity and specificity of the classifiers.

The remaining part of this section introduces a conceptually simple hyperspherical classifier design method that circumvents convergence problems. The proposed approach also provides a systematic procedure for fine-tuning the sensitivity and specificity of the gait recognition system. The design process consists of two phases. The first phase generates a number of hyperspheres to cover all the samples of an enrolled user. The second phase revises the hyperspherical classifier to reduce false rejection error. The procedure for the first phase is:

(1) Divide the samples of the enrolled user (enrolled samples) into two clusters by using the conventional k-means method.
(2) Find the cluster that has the largest number of samples. Replace this cluster by two new clusters which are obtained by clustering the samples associated with the cluster to be replaced into two groups.
(3) With the appearance of new clusters, use the nearest neighbor rule to rearrange the contents of each cluster by computing the distances between every sample and every cluster center.
(4) Continue the process from step 2 until a sufficient number of clusters has been generated.
(5) By using the cluster center as the center and the largest distance between the center and samples belonging to this cluster as the radius, the approach constructs one hypersphere from one cluster. The space occupied by the hyperspheres is chosen as the acceptance region for the enrolled user.

The radius and the center for the ith hypersphere are denoted as R_i and C_i, respectively, in the rest of the paper.

Without considering false acceptance errors, the above procedure achieves a zero false rejection error (and hence, 100% sensitivity) for the training samples. With this result as the starting point, by controlling the false acceptance error, the focus of the second phase of the design process is specificity. By assuming that a sufficient number of samples have been collected from persons that are not enrolled in the biometric system, the following procedure uses such an intruder dataset to refine the hyperspherical classifier.

(1) Let E_i represents the union of the enrolled samples that are encircled by C_i.
(2) Let I_i represents the union of the intruder samples that are contained in C_i.

(3) Let $i = 1$.

(4) Denote P_i as the distance between the center of C_i and the sample contained in E_i that is second farthest away from the center of C_i.

(5) Determine the number of intruder samples that can be removed from I_i if the radius of C_i is reduced to P_i. Note that this operation also excludes the enrolled sample this that is farthest away from C_i from the acceptance region.

(6) Let $i = i + 1$ and continue the process from step 4 until the radius contraction action has been tested for all the hyperspheres.

(7) By assuming C_J to be the hypersphere that has rejected the largest number of intruder samples, reduce the radius of C_J from R_J to P_J.

(8) After updating the contents of E_i and I_i for every hypersphere, repeat this one-hypersphere-at-a-time radius contraction process from step 3 until all the intruder samples have been excluded from the acceptance region encircled by the hyperspheres.

Essentially, the above procedure tries to optimize the cost-effective tradeoffs between sensitivity and specificity. Specifically, by sacrificing one enrolled sample at a time, the method tries to reject as many intruder samples as possible.

In step 7 above, two exceptions require additional treatment. The first exception occurs when more than one hypersphere has rejected the largest number of intruder samples. In this case, the hypersphere that results in the largest reduction of the acceptance region is selected. Theoretically, such a reduction can be measured by $R^M - P^M$, where R and P represent the radii before and after the contraction, respectively, and M is the dimension of the feature space. However, this measure becomes very sensitive to the actual content of the samples when M is large. Therefore, instead of using $M = 50$, which is the dimension of the feature vector employed in this study, M is chosen to be 8 after a number of trial-and-error tests.

The second exception occurs when none of the hyperspheres can reject any intruder sample. In this case, the approach contracts the hypersphere further by choosing parameters P_i as the distance between the center of C_i and the sample contained in E_i that is "third" farthest away from the center of C_i. A similar technique can be repeatedly applied until at least one intruder sample can be rejected from any of the hyperspheres.

4. Experimental results

Knee acceleration signals were collected from 35 subjects divided into user group (5 persons) and intruder group (30 persons). In each data-recording session, the tested subjects were asked to walk normally for forty steps. Members of the intruder group participated in only one data-recording session. Five gait cycles were chosen randomly from these forty steps for fifty times, from which fifty gait feature vectors were generated for each intruder.

Considering the possible day-to-day variation of the walking pattern, members of the enrolled group participated in ten data-recording sessions which were separated by at least one day. By randomly choosing five gait cycles from the 400 recorded gait cycles of each enrolled user for 200 times, 200 gait feature vectors were generated for each member of the user group.

The design process for the hyperspherical classifier was repeated fifty times for each enrolled user. The training dataset consisted of 100 randomly chosen gait samples of the enrolled user and gait samples from 20 randomly selected intruders. The testing dataset included the remaining 100 gait samples of the enrolled user and the gait samples from the remaining ten intruders. Tables

Table 1
Summary of experimental results for one-hypersphere gait recognition system.

Sensitivity	Specificity of the enrolled users				
	1	2	3	4	5
0.95	1.000	0.152	0.277	0.356	0.117
0.90	1.000	0.242	0.359	0.492	0.390
0.85	1.000	0.320	0.417	0.504	0.511
0.80	1.000	0.363	0.446	0.509	0.599
0.75	1.000	0.390	0.489	0.510	0.683
0.70	1.000	0.420	0.569	0.567	0.736
0.65	1.000	0.470	0.745	0.716	0.767
0.60	1.000	0.525	0.889	0.807	0.779
0.55	1.000	0.573	0.943	0.849	0.795
0.50	1.000	0.728	0.960	0.896	0.834

Table 2
Summary of experimental results for 24-hypersphere gait recognition system.

Sensitivity	Specificity of the enrolled users				
	1	2	3	4	5
0.95	0.999	0.783	0.887	0.834	0.835
0.90	1.000	0.897	0.962	0.894	0.890
0.85	1.000	0.931	0.975	0.950	0.946
0.80	1.000	0.945	0.984	0.967	0.965
0.75	1.000	0.952	0.984	0.975	0.992
0.70	1.000	0.955	0.987	0.980	0.993
0.65	1.000	0.956	0.988	0.981	0.994
0.60	1.000	0.962	0.988	0.983	0.994
0.55	1.000	0.964	0.988	0.985	0.994
0.50	1.000	0.970	0.989	0.986	0.994

1 and 2 summarize the averaged experimental results associated with the testing datasets obtained by a single hypersphere classifier (SHC) and a multiple hypersphere classifier (MHC) using 20 hyperspheres. The tables also show how the specificity of the recognition system varies with the sensitivity.

The results of Tables 1 and 2 demonstrate that the MHC outperforms the SHC. For example, by requiring the false rejection error to be no larger than 5% (sensitivity of 0.95), the specificity achieved by the SHC varies from 1.000 to 0.152. In contrast, the specificity of the MHC ranges from 1.000 to 0.783. If we try to improve the specificity by downgrading the sensitivity requirement to 0.80, the specificity of the SHC varies from 1.000 to 0.363, which is still not very satisfactory, but for the MHC the resulting specificity varies from 1.000 to 0.945, which is excellent.

5. Conclusion

This paper presents a gait recognition system for biometric applications based on knee acceleration signals. A feature extraction method has been developed to characterize the walking pattern of different individuals. To distinguish the differences in the walking patterns, a hyperspherical classifier is employed to perform gait recognition. A systematic design method for the hyperspherical classifier has also been developed. The potential of the proposed approach for biometric applications has been demonstrated by experimental results.

To further improve the performance of the gait recognition system, the following directions may be pursued. First, the proposed approach uses a fixed set of feature variable generation rules for every person. To reflect interpersonal differences, a walker-dependent gait feature generation method has the potential to improve the gait recognition rate. Second, this study has not considered the influences of different shoes and different walking surfaces. In order to study the robustness of the gait recognition system, future work may investigate the sensitivity of the performances the

gait recognition system with respect to these uncertainties. Finally, the number of the tested subjects and the time periods for the gait data collection process could be investigated further to fully test the performance of the proposed approach.

References

Andrysek, J., & Chau, G. (2007). An electromechanical swing-phase-controlled prosthetic knee joint for conversion of physiological energy to electrical energy: Feasibility study. *IEEE Transactions on Biomedical Engineering, 54*, 2276–2283.

Araújo, L. C. F., Sucupira, L. H. R., Jr., Liźarraga, M. G., Ling, L. L., & Yabu-Uti, J. B. T. (2005). User authentication through typing biometrics features. *IEEE Transactions on Signal Processing, 52*, 851–855.

Bogert van den, A. J., Read, L., & Nigg, B. M. (1996). A method for inverse dynamic analysis using accelerometry. *Journal of Biomechanics, 29*, 949–954.

Boulgouris, N. V., & Chi, Z. X. (2007). Gait recognition using radon transform and linear discriminant analysis. *IEEE Transactions on Image Processing, 16*, 731–740.

Boulgouris, N. V., Hatzinakos, D., & Plataniotis, K. N. (2005). Gait recognition: A challenging signal processing technology for biometrics. *IEEE Signal Processing Magazine, 22*, 78–90.

Bussmann, J. B., Damen, L., & Stam, H. J. (2000). Analysis and decomposition of signals obtained by thigh-fixed uni-axial accelerometry during normal walking. *Medical and Biological Engineering and Computing, 38*, 632–638.

Chan, A. D. C., Hamdy, M. H., Badre, A., & Badee, V. (2005). Wavelet distance measure for person identification using electrocardiograms. *IEEE Transactions on Instrumentation and Measurement, 57*, 248–253.

Chen, C. H., & Chu, C. T. (2009). High performance iris recognition based on 1-D circular feature extraction and PSO–PNN classifier. *Expert Systems with Applications, 36*, 10351–10356.

Dass, S. C., Zhu, Y., & Jain, A. K. (2007). Validating a biometric authentication system: Sample size requirements. *IEEE Transactions on Pattern Analysis and Machine Intelligence, 28*, 19–30.

Donelan, J. M., Li, Q., Naing, V., Hoffer, J. A., Weber, D. J., & Kuo, A. D. (2008). Biomechanical energy harvesting: generating electricity during walking with minimal user effort. *Science, 319*, 807–810.

Gafurov, D., Snekkenes, E., & Bours, P. (2007). Spoof attacks on gait authentication system. *IEEE Transactions on Information Forensics and Security, 2*, 491–502.

Girgis, M. R., Sewisy, A. A., & Mansour, R. F. (2009). A robust method for partial deformed fingerprints verification using genetic algorithm. *Expert Systems with Applications, 36*, 2008–2016.

Hayes, W. C., Gran, J. D., Nagurka, M. L., Feldman, J. M., & Oatis, C. (1983). Leg motion analysis during gait by multiaxial accelerometry: Theoretical foundations and preliminary validations. *ASME Journal of Biomechanical Engineering, 105*, 283–289.

Hong, J. H., Min, J. K., Cho, U. K., & Cho, S. B. (2008). Fingerprint classification using one-vs-all support vector machines dynamically ordered with naive Bayes classifiers. *Pattern Recognition, 41*, 662–671.

Huang, D. S., Jia, W., & Zhang, D. (2008). Palmprint verification based on principal lines. *Pattern Recognition, 41*, 1316–1328.

Impedovo, D., & Pirlo, G. (2008). Automatic signature verification: The state of the art. *IEEE Transactions on Systems, Man, and Cybernetics, Part C: Applications and Reviews, 38*, 609–635.

Jain, A. K., Ross, A., & Prabhakar, S. (2004). An introduction to biometric recognition. *IEEE Transactions on Circuits and Systems for Video Technology, 14*, 4–20.

Kavanagh, J. J., Morrison, S., James, D. A., & Barrett, R. (2006). Reliability of segmental accelerations measured using a new wireless gait analysis system. *Journal of Biomechanics, 39*, 2863–2872.

Krishnan, S., Rangayyan, R. M., Bell, G. D., & Frank, C. B. (2000). Adaptive time-frequency analysis of knee joint vibroarthrographic signals for noninvasive screening of articular cartilage pathology. *IEEE Transactions on Biomedical Engineering, 47*, 773–783.

Lee, H., Hong, S., & Kim, E. (2009). Neural network ensemble with probabilistic fusion and its application to gait recognition. *Neurocomputing, 72*, 1557–1564.

Mäntyjärvi, J., Lindholm, M., Vildjiounaite, E., Mäkelä, S. M., & Ailisto, H. J. (2005). Identifying users of portable devices from gait pattern with accelerometers. In *Proceedings of the IEEE international conference of acoustics, speech, and signal processing* (pp. 973–976).

McCoy, G. F., McCrea, J. D., Beverland, D. E., Kernohan, W. G., & Mollan, R. A. B. (1987). Vibration arthrography as a diagnostic aid in diseases of the knee. *The Journal of Bone and Surgery*, 288–293.

Nanni, L., Maiorana, E., Lumini, A., & Campisi, P. (2010). Combining local, regional and global matchers for a template protected on-line signature verification system. *Expert Systems with Applications, 37*, 3676–3684.

Nixon, M. S., & Carter, J. N. (2006). Automatic recognition by gait. *Proceedings of the IEEE, 94*, 2013–2024.

Phua, K., Chen, J., Dat, T. H., & Shue, L. (2008). Heart sound as a biometric. *Pattern Recognition, 41*, 906–919.

Rakshit, S., & Monro, D. M. (2007). An evaluation of image sampling and compression for human iris recognition. *IEEE Transactions on Information Forensics and Security, 2*, 605–612.

Rangayyan, R. M., & Wu, Y. F. (2008). Screening of knee-joint vibroarthrographic signals using statistical parameters and radial basis functions. *Medical and Biological Engineering and Computing, 46*, 223–232.

Raudys, S. J., & Jain, A. K. (1991). Small sample size effects in statistical pattern recognition: Recommendations for practitioners. *IEEE Transactions Pattern Analysis and Machine Intelligence, 13*, 252–264.

Sarkar, S., Phillips, P., Liu, Z., Vega, I., Grother, P., & Bowyer, K. (2005). The HumanID gait challenge problem: Data sets, performance and analysis. *IEEE Transactions Pattern Analysis and Machine Intelligence, 27*, 162–177.

Sordo, M., & Zeng, Q. (2005). On sample size and classification accuracy: A performance comparison. *Lecture Notes in Computer Science, 3745*, 193–201.

Su, C. L. (2009). Palm extraction and identification. *Expert Systems with Applications, 36*, 1082–1091.

Tao, D., Li, X., Wu, X., & Maybank, S. (2007). General tensor discriminant analysis and Gabor features for gait recognition. *IEEE Transaction on Pattern Analysis and Machine Intelligence, 29*, 1700–1715.

Telfer, B. A., & Casasent, D. P. (1993). Minimum-cost associative processor for piecewise-hyperspherical classification. *Neural Networks, 6*, 1117–1130.

Wahab, A., Ng, G. S., & Dickiyanto, R. (2005). Speaker authentication system using soft computing approaches. *Neurocomputing, 68*, 13–37.

Wang, L., Leedham, G., & Cho, D. S. Y. (2008). Minutiae feature analysis for infrared hand vein pattern biometrics. *Pattern Recognition, 41*, 920–929.

Wang, J. C., Yang, C. H., Wang, J. F., & Lee, H. P. (2007). Robust speaker identification and verification. *IEEE Computational Intelligence Magazine, 2*, 52–59.

Wu, J. D., & Ye, S. H. (2009). Driver identification using finger-vein patterns with Radon transform and neural network. *Expert Systems with Applications, 36*, 5793–5799.

Xiao, Q. (2007). Technology review-biometrics-technology, application, challenge and computational intelligence solutions. *IEEE Computational Intelligence Magazine, 2*, 5–25.

Xu, D., Yan, S., Tao, D., Zhang, L., Li, X., & Zhang, H. J. (2006). Human gait recognition with matrix representation. *IEEE Transactions on Circuits and Systems for Video Technology, 16*, 896–903.

Yen, C. W. V., & Liu, T. Z. (1997). A competitive learning process for hyperspherical classifiers. *Neurocomputing, 17*, 99–110.

Zhang, R., Vogler, C., & Metaxas, D. (2007). Human gait recognition at sagittal plane. *Image and Vision Computing, 25*, 321–330.

Zhang, D., & Zuo, W. (2007). Computational intelligence-based biometric technologies. *IEEE Computational Intelligence Magazine, 2*, 26–36.